Electronic Supplementary Material (ESI) for Journal of Materials Chemistry A.
This journal is © The Royal Society of Chemistry 2023

Synthesis of Pd–AuAg Trimetal Nanohybrids with Controlled Heterostructures and Their Application in the Continuous Flow Catalytic Reduction of Cr(VI)

Astrini Pradyasti,[a] Hyun Jin Kim,[a] Woo Jin Hyun,[b] and Mun Ho Kim*[a]

[a]Department of Polymer Engineering, Pukyong National University, 45 Yongso-ro, Nam-gu, Busan 48513, Republic of Korea

[b]Department of Materials Science and Engineering, Guangdong Technion − Israel Institute of Technology, 241 Daxue Road, Jinping District, Shantou, Guangdong 515063, China

* Corresponding author: M. H. Kim (munho@pknu.ac.kr)

(Tel.; +82-51-629-6459, Fax; +82-51-629-6429)

Table S1. Comparison of the activity parameter, κ, values for various heterogeneous catalysts, as obtained by dividing the K_{app} by the total weight of the catalysts.

Material	Total weight of catalysts [mg]	K_{app} [min^{-1}]	κ [mg^{-1} min^{-1}]	Ref.
Molybdophosphates	20	0.00351	0.00017	[1]
Pd@polyethyleneimine-modified macadamia nutshell biomass	200	0.038	0.00019	[2]
Ni@interconnected hierarchical carbon	400	0.1564	0.00039	[3]
Nanoscale zero-valent iron–multiwalled carbon nanotube	100	0.053	0.00053	[4]
Volatile suspended solid/Pd	200	0.116	0.00058	[5]
Nanoscale zero-valent iron	41.3	0.0412	0.00099	[6]
Ni@Carbon composites	50	0.1172	0.00234	[7]
Pd nanoparticles/flower-like TiO_2 nanospheres	3	0.00842	0.00280	[8]
Bentonite supported nanoscale zero-valent iron	75	0.2275	0.00303	[9]
PdCu nanoparticles	6	0.0197	0.00328	[10]
Nanoscale zero-valent iron/graphene nanosheets	20	0.075	0.00375	[11]
Magnetic nanoparticles encapsulated in carbonized polydopamine nanospheres/Ag nanoparticles	100	0.474	0.00474	[12]
Fe@C	6	0.045	0.00750	[13]
Thin hydrogel membranes with Pd nanoparticles	5.3	0.045	0.00849	[14]

Pd nanoparticles immobilized on procyanidin-grafted eggshell membrane	15	0.133	0.00886	[15]
Pd/Fe_3O_4 nanocomposites	10	0.09	0.00900	[16]
Nanoscale zero-valent iron supported on herb-residue biochar	50	0.544	0.01088	[17]
Pt nanoparticles immobilized on procyanidin-grafted eggshell membrane	15	0.196	0.01300	[15]
Zero-valent iron@C	40	0.538	0.01345	[18]
Nitrogen-functionalized carbon-doped Pd nanoparticles	8	0.123	0.01537	[19]
Pd@porous polyurea microspheres	7	0.123	0.01757	[20]
Fe_3O_4/Pd nanoparticles	10	0.3	0.03000	[21]
Pd/Fe-mesoporous carbon hybrid nitrogen	8	0.267	0.03337	[22]
Pd@porous polyurea	6	0.25	0.04166	[23]
PdCu nanoboxes	6	0.274	0.04566	[10]
Ni@graphene-Cu composites	4	0.344	0.08600	[24]
Co-rGO	4	0.474	0.11850	[25]
Amino-functionalized Pd nanowires	2	0.282	0.14100	[26]
Montmorillonite supported Fe–Ni bimetallic nanocomposites	2	0.37	0.18500	[27]
Bumpy Pd–AuAg nanohybrids	0.8	0.16163	0.20203	This work

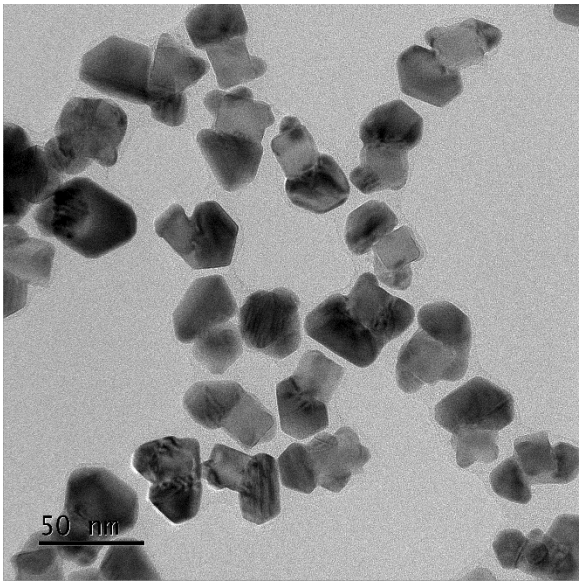

Fig. S1. TEM image of Pd–Au bimetallic nanohybrids obtained after the overgrowth of Au on Pd nanocubes.

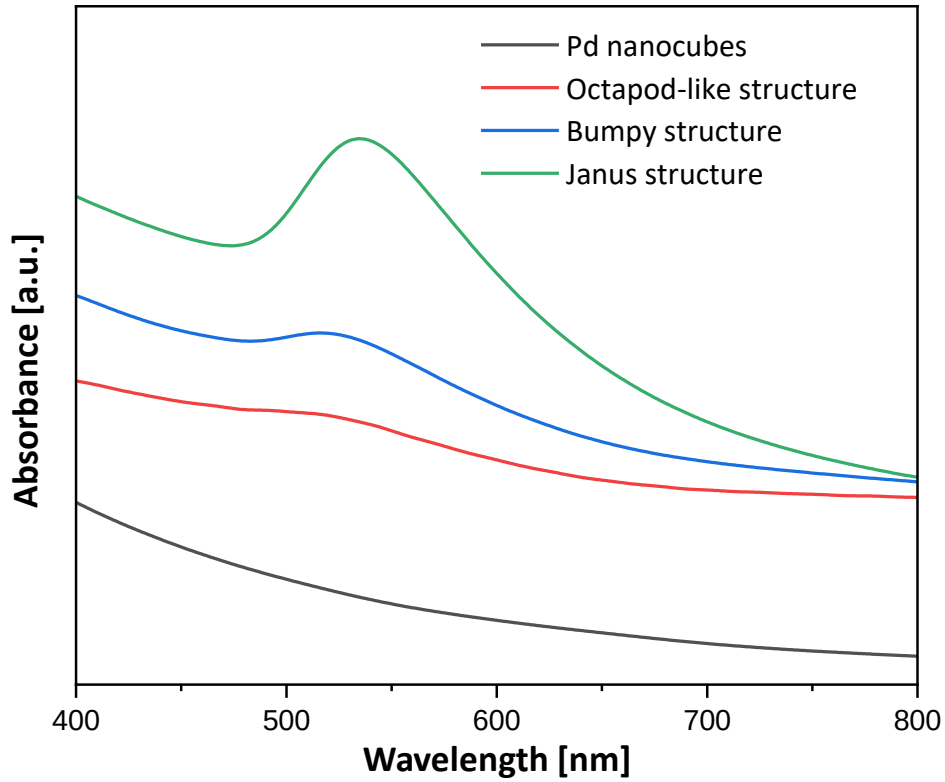

Fig. S2. UV–Vis–NIR spectra of Pd nanocube seeds and Pd–AuAg trimetallic nanohybrids with different heterostructures.

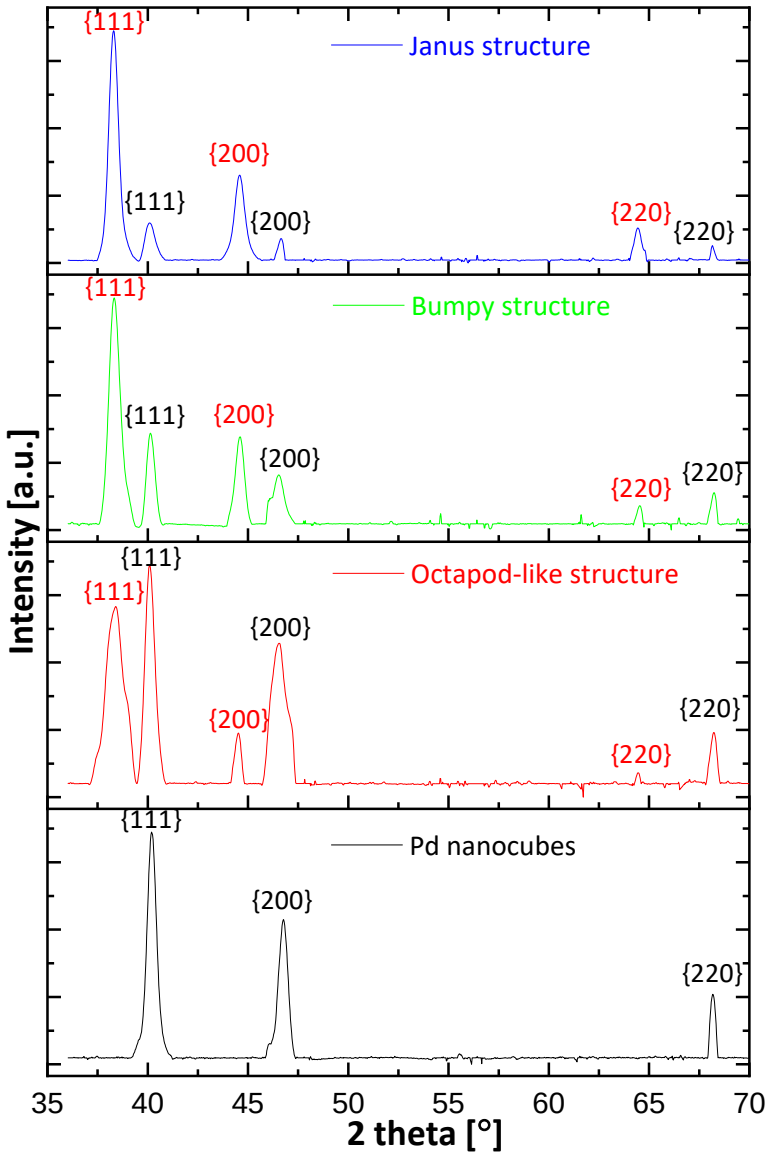

Fig. S3. XRD patterns of Pd–AuAg trimetallic nanohybrids obtained after the seed-mediated growth of Au and Ag on Pd nanocubes.

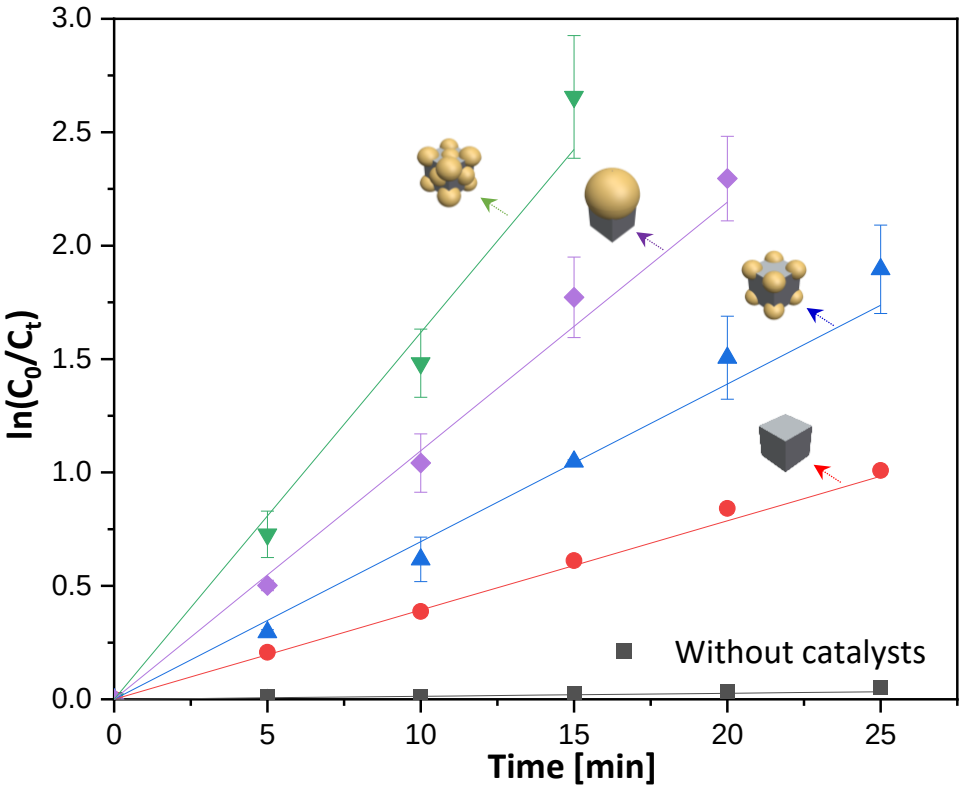

Fig. S4. Reduction kinetics of the Pd nanocubes and Pd–AuAg nanohybrids with different heterostructures for the reduction of Cr(VI) in the presence of formic acid.

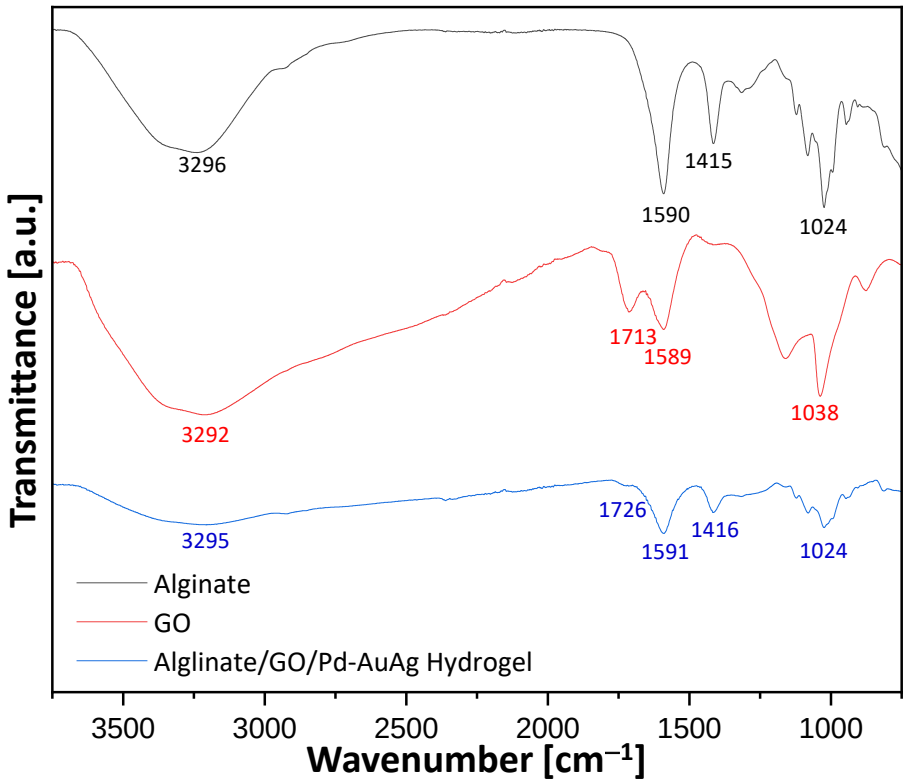

Fig. S5. FTIR spectra of Ca-Alg, GO, and Ca-Alg/GO hydrogel embedded with Pd–AuAg nanohybrids.

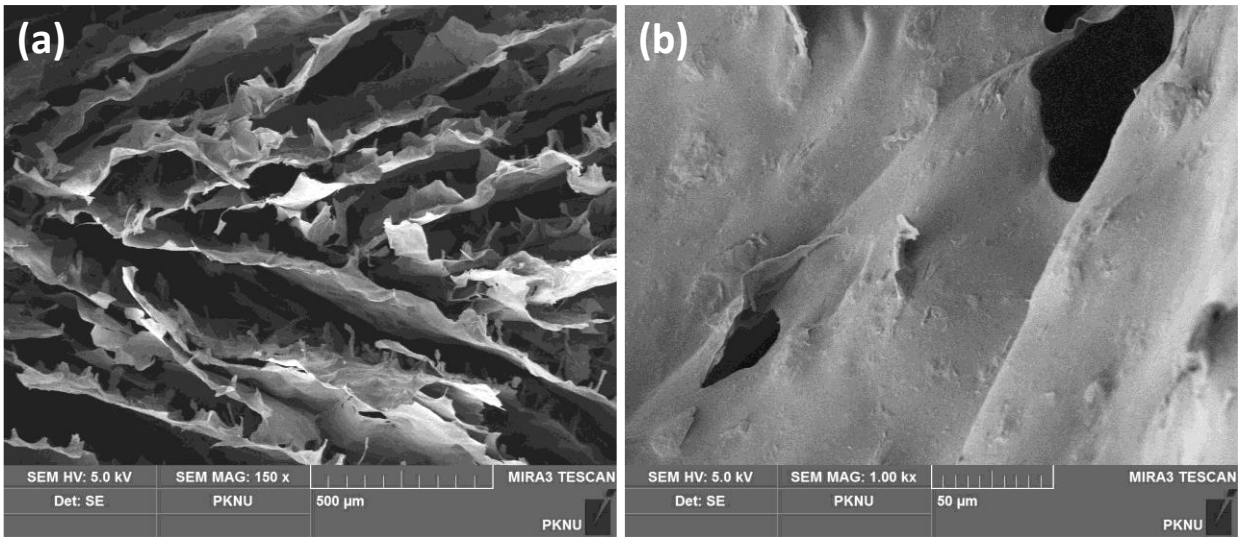

Fig. S6. SEM images of Alg/GO hydrogel embedded with bumpy Pd–AuAg nanohybrids.

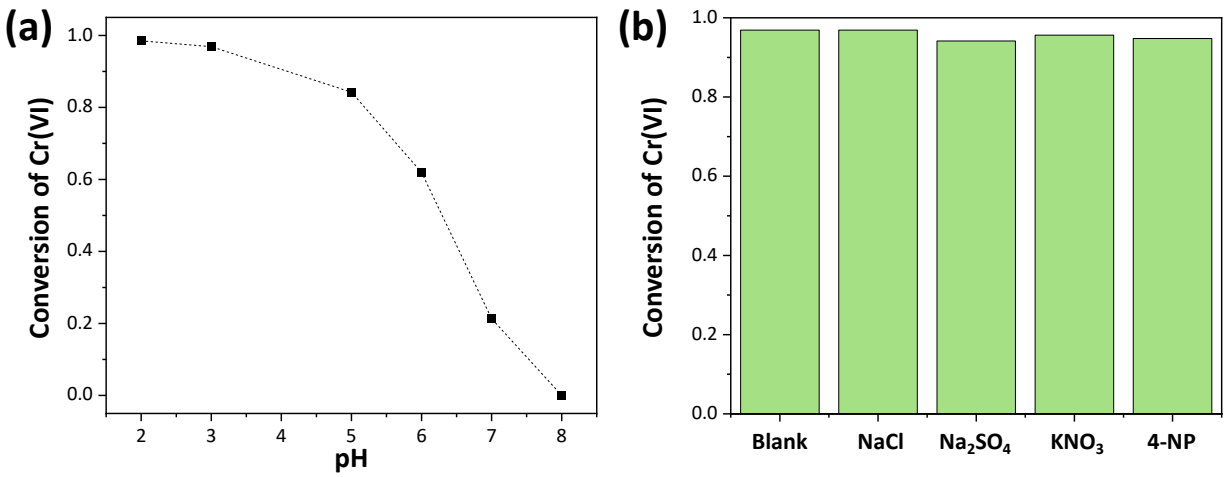

Fig. S7. (a) Cr(VI) conversion in the flow reaction according to pH of reaction aqueous solution. (b) Cr(VI) conversion in the flow reaction in the presence of common anions (such as nitrate, sulfate, and chloride; 10 mM) or 4-nitrophenol (1 mM) in the reaction aqueous solution. The masses of Alg, catalyst (Pd–AuAg nanohybrids), and GO were fixed at 75, 0.8, and 10 mg, respectively, and the flow rate of the reaction mixture was 5 mL/h.

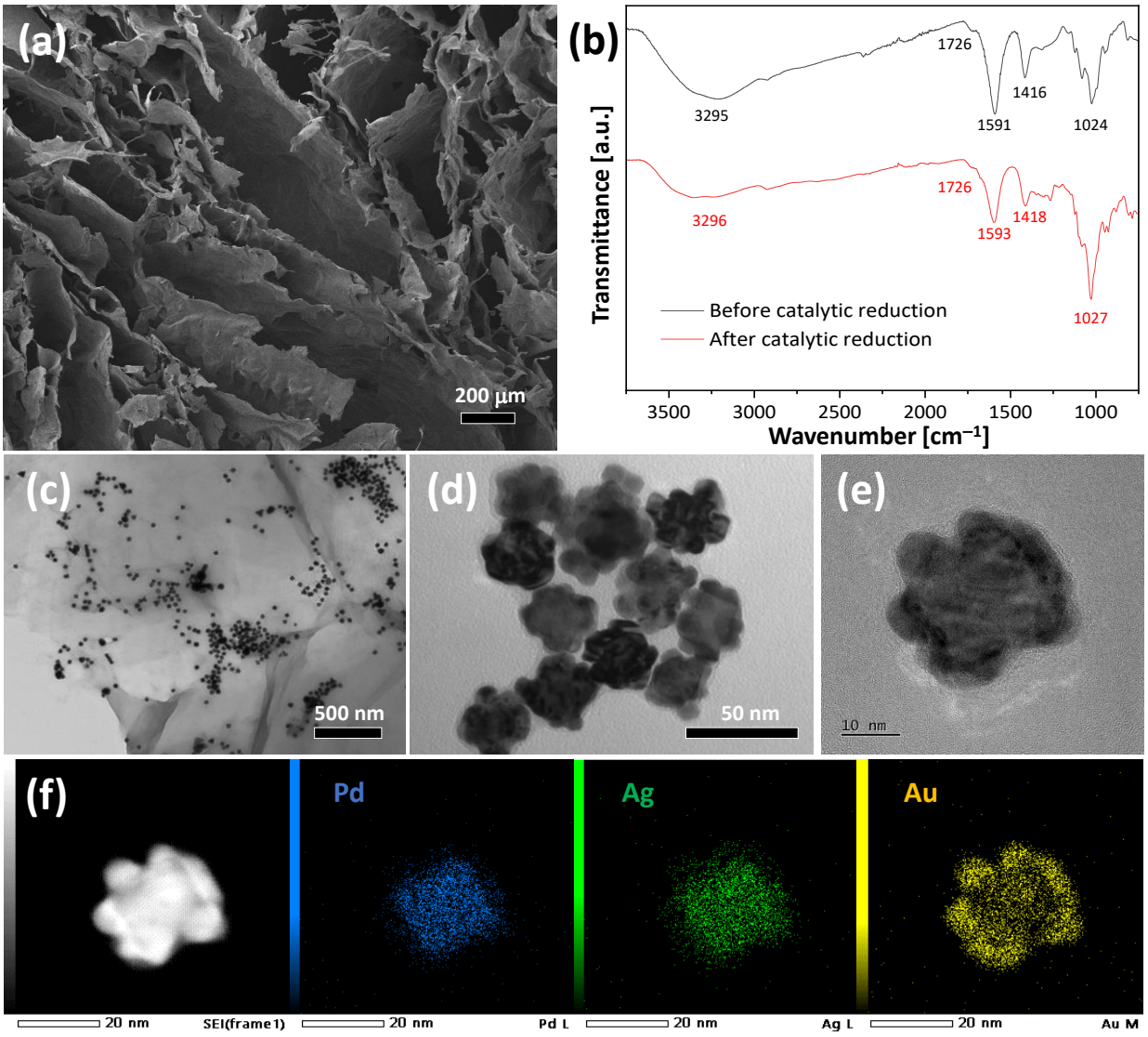

Fig. S8. (a) SEM of the nanocomposite hydrogel after 10 h of continuous reaction. (b) FTIR spectra of the nanocomposite hydrogel before and after 10 h of continuous reaction. (c)–(e) TEM images of the bumpy Pd–AuAg nanohybrids embedded in the nanocomposite hydrogel after 10 h of continuous reaction. (f) Elecmental mapping images of of Pd (blue), Ag (green), and Au (yellow) within a Pd–AuAg nanohybrid.

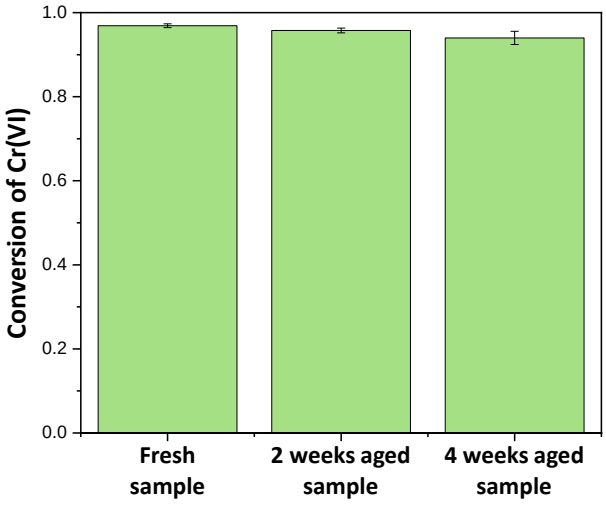

Fig. S9. Cr(VI) conversion in the flow reaction based on the fresh nanocomposite hydrogel and the nanocomposite hydrogels aged 2 and 4 weeks at room temperature in the dried state.

References

1 K. Gong, W. Wang, J. Yan and Z. Han, *J. Mater. Chem. A*, 2015, **3**, 6019–6027.

2 M. Moyo, S. J. Modise and V. E. Pakade, *Sci. Total Environ.*, 2020, **743**, 140614,

3 K. Zhu, L. Chen, N. S. Alharbi and C. Chen, *J. Colloid Interface Sci.*, 2022, **606**, 213–222.

4 X. Lv, J. Xu, G. Jiang and X. Xu, *Chemosphere*, 2011, **85**, 1204–1209.

5 L. Zhou, C. Wu, Y. Xie and S. Xia, *Front. Environ. Sci. Eng.*, , DOI:10.1007/s11783-019-1206-4.

6 F. Fu, J. Ma, L. Xie, B. Tang, W. Han and S. Lin, *J. Environ. Manage.*, 2013, **128**, 822–827.

7 Z. Lv, X. Tan, C. Wang, A. Alsaedi, T. Hayat and C. Chen, *Chem. Eng. J.*, 2020, **389**, 123458.

8 H. Li, M. Gao, Q. Gao, H. Wang, B. Han, K. Xia and C. Zhou, *Appl. Nanosci.*, 2020, **10**, 359–369.

9 L. na Shi, Y. M. Lin, X. Zhang and Z. liang Chen, *Chem. Eng. J.*, 2011, **171**, 612–617.

10 B. Qiao, J. Zhu, Y. Liu, Y. Chen, G. Fu and P. Chen, *CrystEngComm*, 2019, **21**, 3654–3659.

11 X. Li, L. Ai and J. Jiang, *Chem. Eng. J.*, 2016, **288**, 789–797.

12 C. Chen, K. Zhu, K. Chen, A. Alsaedi and T. Hayat, *J. Colloid Interface Sci.*, 2018, **526**, 1–8.

13 Z. Wang, J. Yang, Y. Li, Q. Zhuang and J. Gu, *Eur. J. Inorg. Chem.*, 2018, **2018**, 23–30.

14 I. Sadeghi, E. Y. Liu, H. Yi and A. Asatekin, *ACS Appl. Nano Mater.*, 2019, **2**, 5233–5244.

15 M. Liang, R. Su, W. Qi, Y. Zhang, R. Huang, Y. Yu, L. Wang and Z. He, *Ind. Eng. Chem. Res.*, 2014, **53**, 13635–13643.

16 M. Nasrollahzadeh, Z. Issaabadi and S. M. Sajadi, *Sep. Purif. Technol.*, 2018, **197**, 253–260.

17 J. Shang, M. Zong, Y. Yu, X. Kong, Q. Du and Q. Liao, *J. Environ. Manage.*, 2017, **197**, 331–337.

18 N. Zhou, K. Gong, Q. Hu, X. Cheng, J. Zhou, M. Dong, N. Wang, T. Ding, B. Qiu and Z. Guo, *Chemosphere*, 2020, **242**, 125235.

19 S. Li, L. Tang, G. Zeng, J. Wang, Y. Deng, J. Wang, Z. Xie and Y. Zhou, *Environ. Sci. Pollut. Res.*, 2016, **23**, 22027–22036.

20 M. S. Bashir, *Chem. Eng. Res. Des.*, 2021, **175**, 102–114.

21 X. Tian, M. Liu, K. Iqbal, W. Ye and Y. Chang, *J. Alloys Compd.*, 2020, 826, 154059.

22 M. S. Bashir, X. Jiang, X. Yang and X. Z. Kong, *Ind. Eng. Chem. Res.*, 2021, **60**, 8108–8119.

23 L. Liu, J. Xue, X. Shan, G. He, X. Wang and H. Chen, *Catal. Commun.*, 2016, **75**, 13–17.

24 T. Xu, J. Xue, X. Zhang, G. He and H. Chen, *Appl. Surf. Sci.*, 2017, **402**, 294–300.

25 L. L. Wei, R. Gu and J. M. Lee, *Appl. Catal. B Environ.*, 2015, **176**–**177**, 325–330.

26 B. S. Kadu, Y. D. Sathe, A. B. Ingle, R. C. Chikate, K. R. Patil and C. V. Rode, *Appl. Catal. B Environ.*, 2011, **104**, 407–414.